Low-Frequency Vibrational Excitations in a Niobium-Phosphate Glass for Raman Gain Applications

A. Schulte[1,2,*], Y. Guo[1,2], W. Schirmacher[3], T. Unruh[4], T. Cardinal[5]

[1]Department of Physics and [2]College of Optics & Photonics-CREOL,
University of Central Florida, 4000 Central Florida Blvd., Orlando, FL 32816, USA
[3]Physikdepartment E13 and [4]FRM II, TU München, D-85757 Garching, Germany
[5]ICMCB, CNRS, University of Bordeaux, 33608 Pessac Cedex, France SA

Abstract: Raman gain for all-optical amplification depends significantly on the cross section for spontaneous Raman scattering. We present measurements of the Raman spectrum of binary niobium-phosphate glasses in the frequency range from 5 – 1300 cm^{-1}. The spectra of these glasses show a low-frequency enhancement of the vibrational density of states ('Boson peak') suggesting a significant gain profile for application in Raman amplifiers as well as providing an additional mechanism for Raman gain. To separate the effects of density of states from the light-vibration coupling we carried out an inelastic neutron scattering investigation of 40 Nb_2O_5 - 60 $NaPO_3$ using the time-of-flight spectrometer (TOF-TOF) at the FRM II neutron source in Munich. The Boson peak appears between 40 and 70 cm^{-1} as an increase of the reduced density of states over the flat Debye approximation. Possible mechanisms contributing to the low frequency excitations such as disorder-induced irregular vibrational states are discussed.

Keywords: Raman spectroscopy, Boson peak, Raman gain, neutron scattering

---

[*] Corresponding author. E-mail address: afs@physics.ucf.edu

1. Introduction

Light scattering spectroscopy provides an efficient tool to probe low frequency excitations in glasses and the dynamics of the supercooled liquid [1, 2, 3]. In disordered solids the breakdown of the wave-vector selection rule of crystalline Raman scattering leads to first-order continuous spectra of glasses instead of the discrete Raman spectrum of crystals [1]. The disorder manifests itself in the coupling between the atomic displacements which becomes a random quantity and the fluctuation of the dielectric susceptibility. As compared to the single crystal the vibrational modes are no longer plane waves. The low frequency Raman spectrum of glasses may be attributed to two main contributions: a quasi-elastic component usually assigned to the presence of very fast (subpicosecond) relaxation processes [1, 4, 5] and the vibrational part or the so-called Boson peak [2, 5]. The low frequency excitations in the spectral region of the Boson peak and the associated vibrational density of states are the focus of this paper. Glasses with broad and intense Raman active modes have recently attracted increased attention as gain materials for optical communication systems [6]. A direct comparison between spontaneous and Raman gain spectra in two Tellurium-oxide glasses has shown a peak gain thirty times that of fused silica and twice its spectral bandwidth [7]. It was also demonstrated that the Raman gain profile and intensity mimics that of the spontaneous Raman spectrum. In the frequency range below 200 cm^{-1} intense Raman scattering is observed in the Tellurium oxide glasses [8] as well as in the niobium phosphate glasses which are the focus of the present study. It indicates that in the these glasses a nearly frequency independent Raman gain profile down to very low wavenumber can be obtained while the gain is more than ten times that of fused silica. There are several mechanisms which may contribute to the low frequency Raman band including localized vibrational states and disorder-induced irregular vibrational states ('Boson peak') [9, 10, 11], and our objective is to investigate their role. The density of vibrational states information, however, is hidden in the Raman spectrum because of the light-vibration coupling coefficient's dependence on frequency. Therefore inelastic Neutron Scattering (INS) experiments are conducted on a niobium phophate glass to extract the one-phonon vibrational density of states. Through combined analysis of the Raman and the inelastic neutron scattering spectra the light-vibration coupling coefficient is determined within the approximation of the Shuker-Gammon model [12] for the Raman scattering cross section.

2. Experimental

The niobium phosphate glasses were elaborated from $NaPO_3$ and Nb_2O_5 raw material using standard melting methods at 1100 °C in platinum crucibles [13]. After quenching the glasses were annealed for 15 hours at 30 °C below their glass transition temperature (670 °C for 40 Nb_2O_5 - 60 $NaPO_3$) .

For the spontaneous Raman measurements an Argon ion laser (λ = 514.5 nm) operating in single mode was employed as the excitation source. A polarizer and half-wave plate combination was used to select the polarization direction (vertical, v, or horizontal, h) of the scattered light. The Raman signal was collected in a backscattering geometry and spectrally analyzed at a resolution of 1 cm^{-1} with a scanning double monochromator (U1000, JY Horiba) which was equipped with a photomultiplier detector and a single photon counting system.

Thermal neutron scattering experiments were carried out at the time-of-flight spectrometer TOF-TOF at the Munich neutron source FRM II at an incident wavelength of 4.7 Å with an energy resolution of 0.1 meV. The 40 Nb_2O_5 - 60 $NaPO_3$ glass in powder form was filled in Nb double-cylinders with 0.1 mm wall thickness. Inelastic neutron scattering spectra were measured at room temperature. A vanadium standard in the same geometry was used to correct for detector efficiencies.

3. Results and Discussion

The spontaneous Raman spectra over the frequency range from 6 to 1300 cm^{-1} are shown in Fig. 1. For both vv and vh polarizations, an intense low frequency peak is visible on the Stokes as well as on the Anti-Stokes side. This peak is attributed to excess vibrational density of states in the amorphous solid after correction of the scattered intensity for the thermal population factor (see Fig. 2).

The bands in the frequency range above 130 cm^{-1} are attributed to molecular vibrations as opposed to the Boson peak. The peak around 910cm^{-1}, due to the isolated Nb-O vibration [14], is very prominent in the sample containing 20% Nb_2O_5, i.e. for lower niobium concentration. The increase of Nb_2O_5 concentration to 40% gives rise to bands around 830 cm^{-1} and 650 cm^{-1} [14, 15]. The band at 830 cm^{-1} suggests the formation of corner shared NbO_6 octahedral chains. The band at 650 cm^{-1} is related to the formation of a three-dimensional framework implying less distorted octahedral similar to a tungsten bronze structure [14]. The 266 cm^{-1} peak in the glass with 20% Nb_2O_5 is associated with vibrational modes involving bending and torsional vibrations of the phosphate network. In the sample containing 40% Nb_2O_5 this peak is shifted to lower frequency which may be attributed to the larger mass of niobium compared to phosphorous.

In Fig. 2 relevant representations of the low frequency Raman spectrum of the 40 Nb_2O_5 - 60 $NaPO_3$ glass on the Stokes side are shown. These are the measured intensity, the Raman susceptibility, and the reduced Raman intensity. In the low frequency range the scattered intensity needs to be corrected for the thermal population factor $n(\nu)+1$, where $n(\nu,T)$ = [exp (hν/kT) − 1], ν is the frequency, T the temperature, and h and k are Planck and Boltzmann constants. The vv polarized spectra divided by n(ν)+1 are shown in the mid panel of Fig. 2. These correspond to the Raman susceptibility and thus to the Raman gain curves predicted from the spontaneous scattering [15]. They deviate from the Raman intensity spectra in the low frequency range where the correction from the Bose-Einstein factor dominates. Shuker and Gammon [12] derived an expression which is commonly used to connect the low frequency Raman scattering in amorphous solids with the vibrational density of states.

$$I_{Rr}(\nu) = \frac{I_R(\nu)}{[n(\nu)+1]\nu} \propto C(\nu)\ \frac{g(\nu)}{\nu^2} \qquad (1)$$

Here, g(ν) is an effective vibrational density of states as function a of frequency ν. The coupling of light to vibrational excitations is described by a frequency dependent function C(ν). In equ. (1) spatial correlations of vibrations over distances longer than the wavelength of light or phonon eigenstates are neglected. Thus C(ν) is treated as a phenomenological quantity which is determined experimentally by comparing the Raman data with independently measured neutron spectra.

From Fig. 2 it is evident (bottom curve) that the reduced Raman intensity $I_{Rr}(\nu)$ shows an enhancement over the Debye density of states, assuming a monotic variation of C(ν). The prominent 'Boson' peak near 65 cm^{-1}, which is the main reason for the performnce of our materials as Raman amplifiers in the low frequency range, has been observed in a large number of disordered materials. The origin of the low-frequency enhancement of the density of states of disordered materials has been discussed quite controversely in the literature. Karpov, Ignat'ev and Klinger [16] have established the soft-potential model, which postulates the existence of local anharmonic structural defects, which are supposed to interact with acoustic phonons. The hybridization of these defect states with the phonons are made responsible for the Boson peak. Other authors [10, 17, 18] postulate the existence of additional localized vibrational states in the Boson peak range. Another approach to explaining the Boson peak has been put forward by Goetze and Mayr [19], who extended the mode-coupling theory of the liquid-glass transition into the glassy regime. In this regime the dynamics is shown to be mainly harmonic in character and exhibits a so-called anomalous vibrational peak, which was related to the Boson peak. A fourth group assumed a distribution of harmonic force constants, produced by the structural disorder. Comparing a computer simulation with a coherent potential approximation (CPA) they showed that the boson peak appears as the low-frequency edge of a disorder-induced band of irregular vibrational states which obey random-matrix statistics. The features of this statistics pointed to a delocalized nature of the states in the Boson peak regime [20]. More recently, this approach has been generalized in several ways: The theory has been formulated as a generalized elasticity theory in which the disorder is postulated to lead to spatially fluctuating elastic constants. It encompasses a full vector character of the vibrational excitations. The theory has been extended to be applicable to calculate the thermal conductivity, and a causal relationship between the Boson peak and the plateau in its temperature dependence has been established [21]. This suggests that it is the state of frozen-in disorder of the materials which produces the Boson peak and is, therefore, crucial for having a favorable Raman gain at low frequencies.

From the Raman spectra alone, it is not possible to obtain directly the density of states using the Shuker-Gammon equation (1), because it also contains the light-vibration coupling function $C(\nu)$. $C(\nu)$ measures the average scattering efficiency of the vibrational modes with frequency between ν and $\nu + d\nu$. In principle, not even neutron scattering does supply the true $g(\nu)$, because of the different scattering amplitudes of the atomic components. However, using the incoherent approximation, the inelastic neutron scattering intensity I_N in glasses can be connected to the vibrational density of states g(ν) by a similar equation [22, 23, 24], but which does not contain the light-vibration coupling function.

$$I_{Nr}(\nu) = \frac{I_N(\nu)}{[n(\nu)+1]\nu} \propto \frac{g(\nu)}{\nu^2} \qquad (2)$$

To obtain information on the vibrational dynamics in the 40 Nb_2O_5 - 60 $NaPO_3$ glass we carried out an inelastic neutron scattering experiment using the time-of-flight spectrometer (TOF-TOF) of the FRM II in Munich. The constituents of our material are all coherent scatterers of similar cross section. By averaging over the full accessible scattering angle (wavevector) range we obtain a g(ν) which gives an approximate spectral distribution of the vibrational modes. The time-of-flight data underwent the usual correction procedure such as correction for the detector efficiencies, normalization to a vanadium scan, and subtraction of the empty cell contribution. The density of states was obtained by an iterative procedure after correcting for the Debye-Waller factor and multiphonon contributions.

The resultant density of states g(ν) and $g(\nu)/\nu^2$ at 295 K are shown in Fig. 3 and in the middle panel of Fig. 4, respectively. The Boson peak appears between 40 and 70 cm^{-1} as an enhancement of the reduced density of states over the Debye approximation. In Fig. 4, the reduced Raman scattering intensity is also plotted (top panel). The light-vibration coupling coefficient is then obtained as the ratio of these two data sets, according to equs. (1) and (2), and shown in the bottom panel of Fig. 4.

The linear increase of the coupling coefficient as a function of frequency between 40 and 120 cm^{-1} is clearly seen in the plot. A linear frequency dependence has been reported for a wide range of amorphous systmes [24, 25]. The linear increase of the coupling coefficient C(ν) with frequency suggests that the origin of the Boson peak is not purely due to localized vibrations, but includes diffusional modes [26]. It remains a challenge for the theory to go beyond the Shuker-Gammon expression for the Raman scattered intensity in amorphous systems and to include correlations over distances longer than the wavelength of light and phonon eigenstates.

4. Conclusions

In conclusion, we have measured the enhancement of low frequency vibrational modes (Boson peak) in a binary niobium phosphate glass, which provides a mechanism for significant Raman gain in the low frequency region. The density of vibrational states in the incoherent approximation and the light-vibration coupling coefficient have been derived from combined Raman and neutron scattering data. The coupling coefficient shows a linear increase with frequency in the Boson peak region which suggests that it is not purely due to localized vibrations.

Acknowledgments: We thank W. Petry for support at the Technical Univesity of Munich. This work was supported in part by NSF grants ECS-0123484 and DMR-0421253, by the Agence Nationale de la recherche ANR (grant ANR-05-BLAN-0212-01), and by the new neutron source FRM II through the allocation of beam time.

References

[1] J. Jäckle, “ Low Frequency Raman Scattering in Glasses”, in Amorphous Solids, Ed. W. A. Phillips, (Springer, 1981) 135.

[2] C. Carabatos-Nedelec, “Raman Scattering of Glass”, in Handbook of Raman Spectroscopy, Eds. I. R. Lewis, H. G. M. Edwards, (Marcel Dekker, 2001) 423.

[3] H.Z. Cummins, G. Li, W.M. Du, and N.J.Tao, J. Phys. Condens. Matter 6 (Supp. 23A) (1994) A51.

[4] G. Winterling, Phys. Rev. B12 (1975) 2432.

[5] S. N. Yannopoulos, D. Th. Kastrissios, Phys. Rev. E 65 (2002) 021510.

[6] M. Islam, “Raman Amplifiers for Telecommunications 1: Physical Properties” (Springer, 2004).

[7] R. Stegeman, L. Jankovic, H. Kim, C. Rivero, G. Stegeman, K. Richardson P. Delfyett, Y. Guo, A. Schulte, T. Cardinal, Optics Letters 28 (2003) 1126.

[8] Y. Guo, S. Nonnenmann, A. Schulte, C. Rivero, K. Richardson, R. Stegeman, G. Stegeman, T. Cardinal, Conference on Lasers and Electro-Optics Technical Digest (OSA) (2004) CThP2.

[9] R.S. Krishnan, Proc. Indian Acad. Sci. A 37 (1953) 377.

[10] J. Graebner, B. Golding, L. Allen, Phys. Rev. B 34 (1986) 5696.

[11] S. R. Elliott, “Amorphous Materials: Boson Peak”, in Encyclopedia of Materials: Science and Technology (Elsevier, 2005) 171.

[12] R. Shuker, R. W. Gammon, Phys. Rev. Lett. 25 (1970) 222.

[13] T. Cardinal, E. Fargin, G. Le Flem, M. Couzi, L. Canioni, P. Segonds, L. Sarger, A. Ducasse, F. Adamietz, Eur. J. of Solid State and Inorg, Chem. 33 (1996) 597.

[14] T.Cardinal, E. Fargin, G. Le Flem, S. Leboiteux, J. Non-Crystal. Solids 222 (1997) 228.

[15] Y. Guo, A. Schulte, R. Stegeman, G. Stegeman, C. Rivero, K. Richardson, T. Cardinal, Conference on Lasers and Electro-Optics Technical Digest (OSA) (2005) CME2.

[16] V. G. Karpov, M. I. Klinger, F. N. Ignatiev, Sov. Phys. JETP 57 (1983) 439.

[17] S. R. Elliott, Europhys. Lett. 19 (1992) 201.

[18] S. N. Taraskin, Y. L. Loh, G. Natarajan, S. R. Elliott, Phys. Rev. Lett. 86 (2001) 1255.

[19] W. Götze, M. R. Mayr, Phys. Rev. E 61 (2000) 587.

[20] W. Schirmacher, G. Diezemann, C. Ganter, Phys. Rev. Lett. 81 (1998) 136.

[21] W. Schirmacher, Europhys. Lett. 73 (2006) 892.

[22] J.M. Carpenter, and C.A. Pelizzari, Phys. Rev. B 12 (1975) 2391.

[23] U. Buchenau, Z. Phys. B 58 (1985) 181.

[24] A. Fontana, F. Rossi, G. Villani, S. Caponi, E. Fabiani, G. Baldi, G. Ruocco, R. Dal Maschio, J. Phys.: Condens. Matter 19 (2007) 205145.

[25] N. V. Surovtsev, A. P. Sokolov, Phys. Rev. B 66 (2003) 054205.

[26] N. V. Surovtsev, S. V. Adichtchev, E. Rössler, M. A. Ramos, J. Phys.: Condens. Matter 16 (2004) 223.

Figure Captions

Fig. 1 Raman spectra of 40 Nb_2O_5 – 60 $NaPO_3$ (top) and 20 Nb_2O_5 – 80 $NaPO_3$ (bottom) glasses excited at a wavelength of 514.5 nm. Shown are polarized and depolarized spectra on both the Stokes and Anti-Stokes sides. Note that the Stokes shift is shown in the negative wavenumber direction.

Fig. 2 Intensity of Raman scattering (Stokes side) in 40 Nb_2O_5 – 60 $NaPO_3$ glass in three different representations: Raman intensity (top), Raman susceptibility (middle), and reduced Raman intensity (bottom).

Fig. 3 Low-frequency vibrational density of states of 40 Nb_2O_5 – 60 $NaPO_3$ glass determined from thermal neutron scattering.

Fig. 4 Frequency dependence of vibrational properties in the Boson peak region of 40 Nb_2O_5 – 60 $NaPO_3$ glass:

(top) Reduced Raman intensity $g(\nu) / \nu^2 C(\nu)$ in Shuker-Gammon representation (see text)

(middle) Reduced vibrational density of states $g(\nu) / \nu^2$ from neutron scattering.

(bottom) Light-vibration coupling coefficient $C(\nu)$. The linear frequency dependence is indicated by the straight line.

Fig. 1

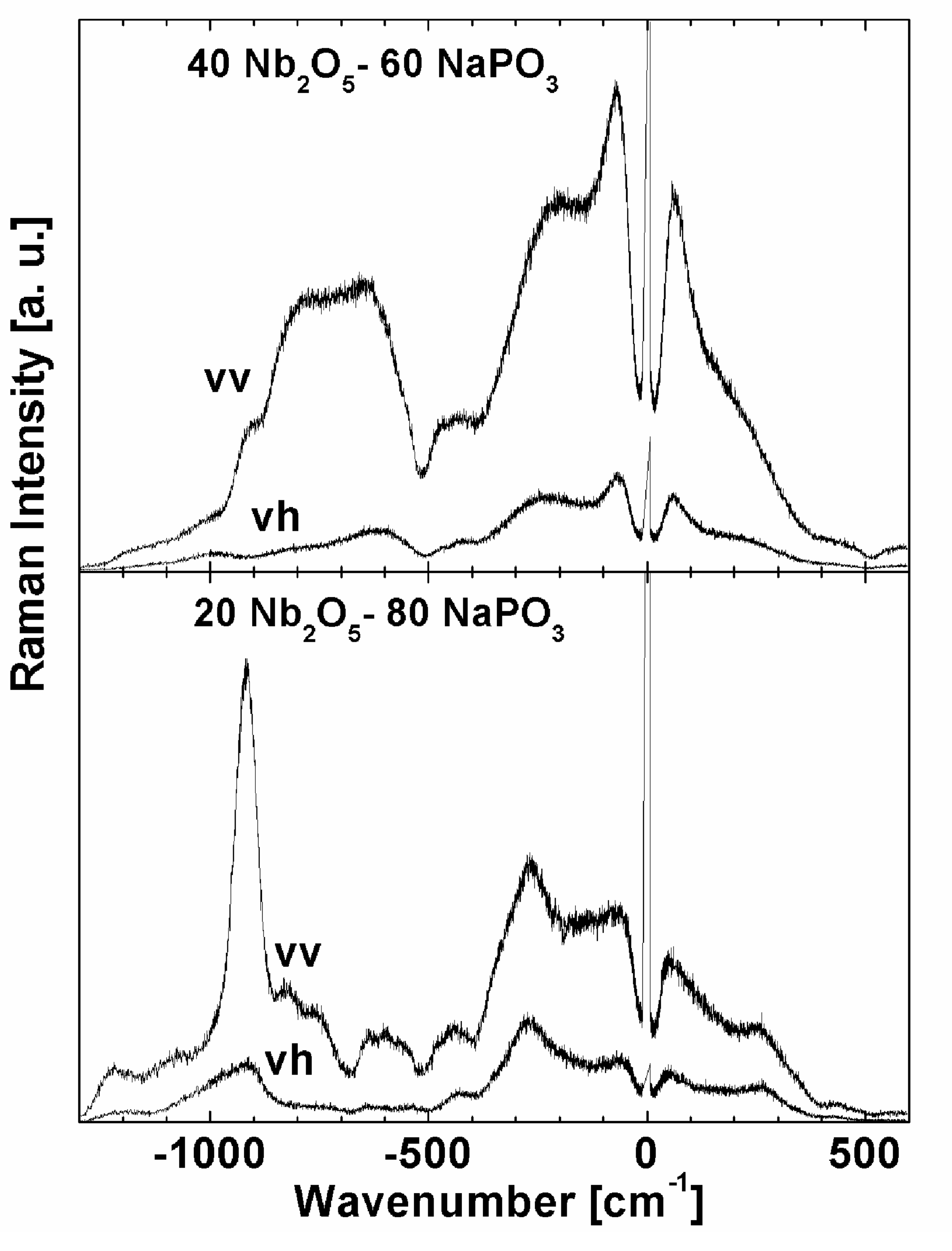
40 Nb_2O_5- 60 $NaPO_3$
vv
vh
20 Nb_2O_5- 80 $NaPO_3$
vv
vh
Raman Intensity [a. u.]
-1000
-500
0
500
Wavenumber [cm^{-1}]

Fig. 2

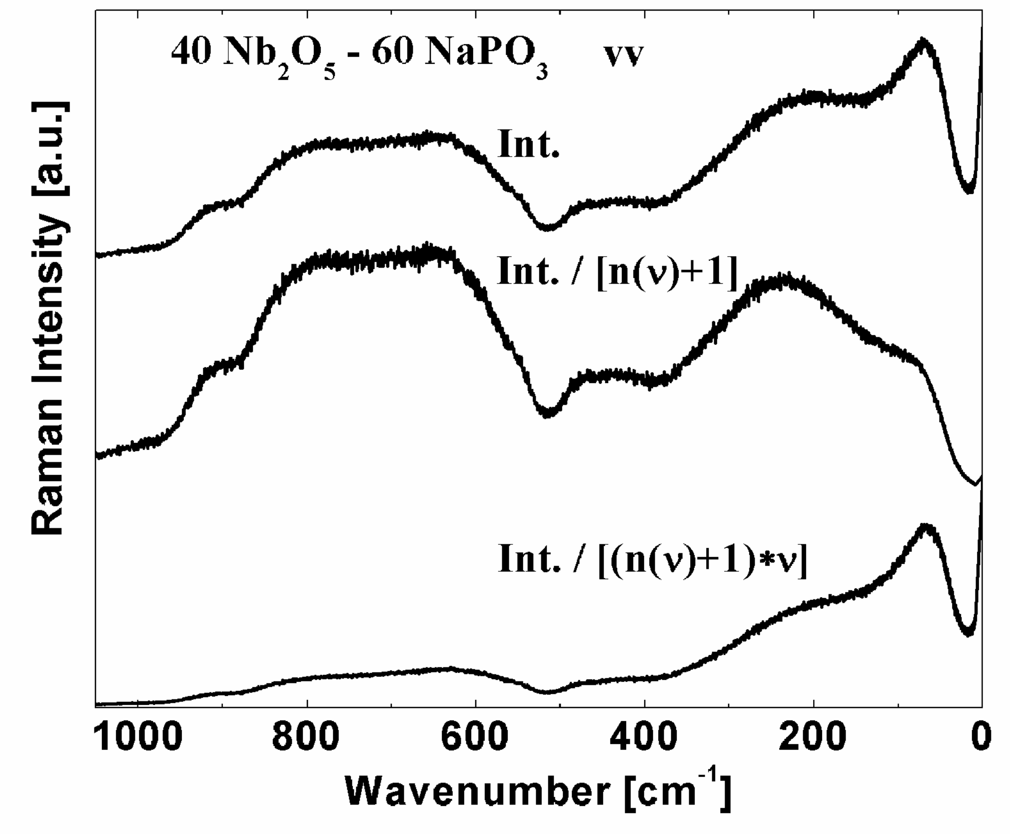

40 Nb2O5 - 60 NaPO3 vv
Int.
Int. / [n(ν)+1]
Int. / [(n(ν)+1)*ν]
Raman Intensity [a.u.]
1000
800
600
400
200
0
Wavenumber [cm-1]

Fig. 3

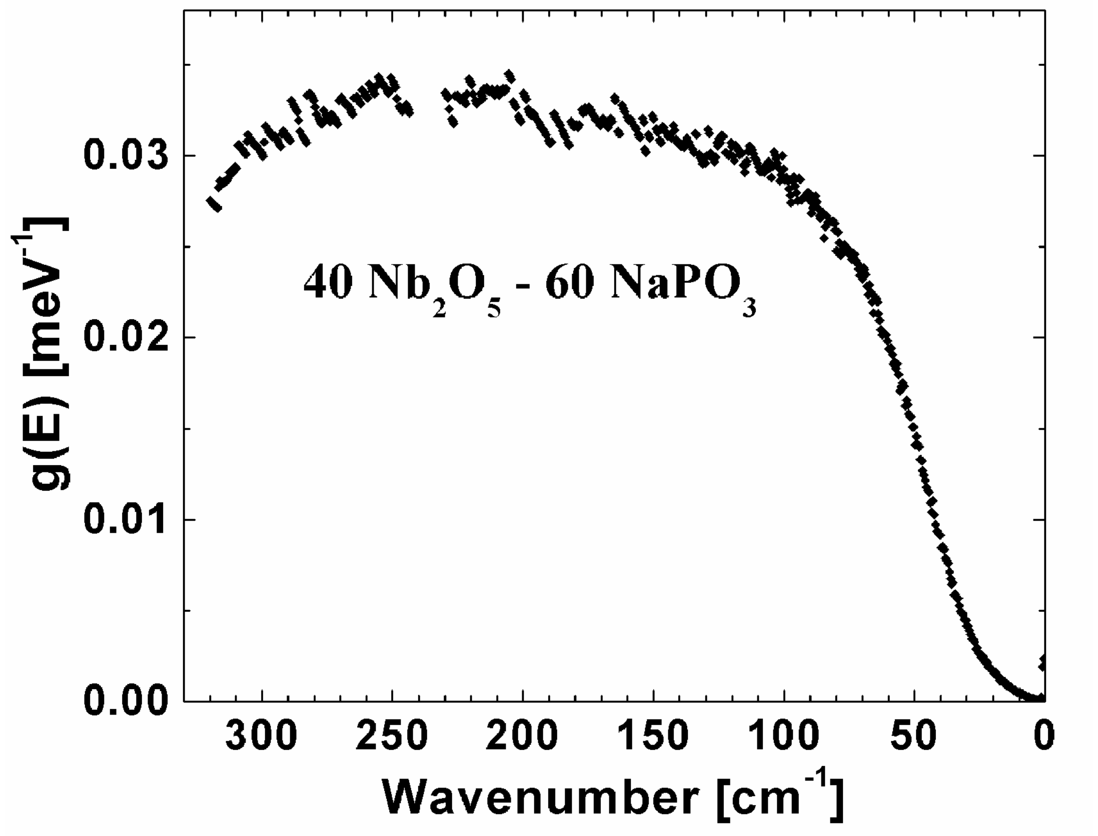
40 Nb_2O_5 - 60 $NaPO_3$
g(E) [meV^{-1}]
0.00
0.01
0.02
0.03
Wavenumber [cm^{-1}]
300
250
200
150
100
50
0

Fig. 4

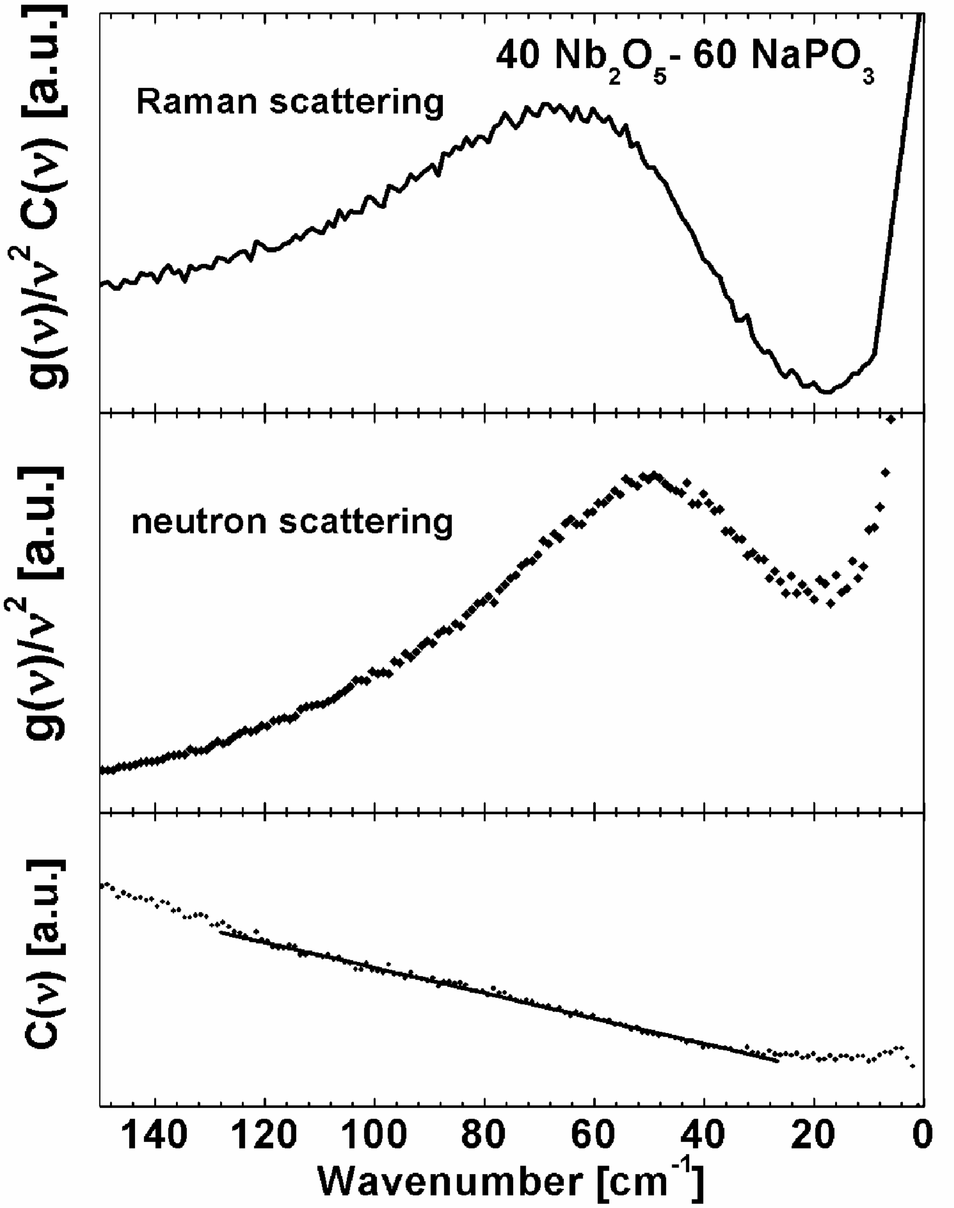
40 Nb$_2$O$_5$- 60 NaPO$_3$
Raman scattering
g(ν)/ν^2 C(ν) [a.u.]
neutron scattering
g(ν)/ν^2 [a.u.]
C(ν) [a.u.]
140
120
100
80
60
40
20
0
Wavenumber [cm^{-1}]